


## ORIGINAL ARTICLE

# An integrated experimental-computational study of the microclimate under dressings applied to intact weight-bearing skin

Dafna Schwartz | Amit Gefen 

Department of Biomedical Engineering,  
Faculty of Engineering, Tel Aviv  
University, Tel Aviv, Israel

## Correspondence to

Amit Gefen, PhD, Professor of Biomedical  
Engineering, The Herbert J. Berman  
Chair in Vascular Bioengineering,  
Department of Biomedical Engineering,  
Faculty of Engineering, Tel Aviv  
University, Tel Aviv 6997801, Israel.  
E-mail: gefen@tauex.tau.ac.il

## Funding information

Ferris Mfg. Corp., Fort Worth TX, USA,  
Grant/Award Number: This work was  
supported by an unrestricted educati

## Abstract

Pressure ulcers (PUs) are one of the most prevalent adverse events in acute and chronic care. The root aetiological cause of PUs is sustained cell and tissue deformations, which triggers a synergistic tissue damage cascade that accelerates over relatively short time periods. Changes in skin microclimate conditions are known to indirectly contribute to PU-risk levels or to exacerbation of existing wounds. It is therefore surprising that information concerning heat accumulation under dressings is poor. Here, we aimed to investigate the effects of dressings on the microclimate of weight-bearing buttocks skin in 1-hour supine lying sessions. Using a novel and originally developed experimental-computational approach, we compared the combined influence of the mechanical and thermal properties of a polymeric membrane dressing (PolyMem, Ferris Mfg. Corp., Fort Worth, TX) on skin microclimate under and near the dressings with those of a standard placebo foam dressing. We specifically identified the *thermal conductivity* properties of dressings as being highly important in the context of protective dressing performances, given its association with potential heat accumulation under dressings. Accordingly, this article highlights, for the first time in the literature, the relevance of thermal properties of a dressing in effectively mitigating the risk of developing PUs or aggravating an injury, and offers a systematic, methodological bioengineering process for assessing the thermal performances of dressings.

## KEYWORDS

finite element method, heat accumulation, multiphysics computational modelling, pressure ulcer prophylaxis

## 1 | INTRODUCTION

Pressure ulcers (PUs), also often called pressure injuries, are one of the most prevalent and adverse events in acute

**Abbreviations:** 3D, three-dimensional; COF, coefficient of friction; DTI, deep tissue injury; FE, finite element; IRT, infrared thermography; MRI, magnetic resonance imaging; PHCI, protective heat clearance index; PMD, polymeric membrane dressing; PU, pressure ulcer; RCT, randomised clinical trial; ROI, region of interest; SC, stratum corneum; TEH, temperature exposure histogram; VOI, volume of interest.

and chronic healthcare facilities. To minimise their occurrence that not only cause human suffering but also impose high financial burden and litigation risks, healthcare organisations, governments, industry, and academia are now focusing more on PU prevention in addition to treatment.

The root aetiological cause of PUs, both the ones associated with prolonged exposure to bodyweight forces and those formed in connection with the use of skin-contacting or force-applying medical devices (so called

'medical device-related pressure ulcers'), is sustained cell and tissue deformations.<sup>1,2</sup> The sustained cell and tissue deformations result in direct cell damage, and then, typically, secondary inflammatory damage, to which tertiary ischaemic damage is later added, in a synergistic cascade that accelerates over a relatively short time course of tens of minutes to hours.<sup>1,2</sup> The tissue damage in a forming PU may start internally, under intact skin, at which phase it is termed a deep tissue injury (DTI), which may eventually progress to a full-thickness wound. The damage process is also possible in the opposite direction, where an epidermal-dermal injury progresses towards the depth of the tissues and spreads internally, and eventually, evolves into a deep PU.<sup>2</sup> In either route of PU pathogenesis, the structure and function of skin play a pivotal role.

The morphological and mechanical properties of skin are influenced by numerous factors, including age, health status, and diseases, and such effects can be systemic (ie, over the entire skin organ) or local, as in a burn, scar, or site of a lesion. Focusing on potential localised effects on skin structure and function, the thermodynamic environment including the local (i) skin temperature, (ii) humidity at the vicinity of skin, and (iii) air movement near the skin will have a substantial impact on skin properties and behaviour.<sup>3</sup> These last three factors define the skin microclimate conditions at a certain body site. Changes in skin microclimate conditions, that is, fluctuation of one or more of the three aforementioned factors outside their respective neutral ranges, will very likely compromise skin functionality and tolerance to mechanical loads, thereby indirectly contributing to a PU risk.<sup>3-5</sup>

The localised temperature and humidity of skin are strongly coupled with the state of skin and subdermal tissue deformations and mechanical stresses. The stratum corneum (SC), being the outermost skin layer, is the first to be affected by microclimate changes. Moisture and wetness, for example, due to prolonged skin occlusion by an impermeable material, or when a patient is exposed to incontinence, lead to SC hydration, which remarkably and promptly decreases the stiffness and strength of the SC.<sup>6-8</sup> Moreover, when the skin is moist at a certain region, the coefficient of friction (COF) between that skin region and any contacting material (eg, clothing, garments, diaper, bedsheets, or a support surface) increases, leading to more adherence of skin to the contacting object, and, hence, to greater deformations and stresses, primarily in shear, within cutaneous and subcutaneous tissues.<sup>9</sup> Skin moisture therefore leads to lower tissue strength and stiffness and, at the same time, to increased mechanical loading (by elevated frictional forces), which concurrently increase the risk to (either superficial or subdermal) PUs. Skin dryness, on the other hand, is also

### Key Messages

- changes in skin microclimate conditions are known to indirectly contribute to pressure ulcer risk levels or to exacerbation of existing wounds, hence it is surprising that information concerning heat accumulation under dressings is poor
- using a novel experimental-computational approach, we compared the combined influence of the mechanical and thermal properties of a polymeric membrane dressing on skin microclimate, under and near the dressing, with those of a standard placebo foam dressing
- our data confirmed that skin and subdermal tissue temperatures rise, and that heat is naturally being accumulated at the contact areas between the weight-bearing buttocks and dressing or a support surface
- our experimental-computational results, considered together, demonstrated that the thermal, physical, and mechanical properties of the materials that are in contact with skin have a distinguished impact on the resulted skin temperature rise

undesirable, as it increases fragility and susceptibility to cracks and fissures, which from a biomechanical perspective also promote tissue stress concentrations that may lead to superficial PUs.<sup>10-14</sup> Accordingly, hydration of the SC needs to be regulated and be continuously maintained within a normative range for the PU risk to be kept minimal.

The localised skin temperature is an important factor contributing to the corresponding skin moisture. Locally elevated skin temperatures drive local perspiration, whereas locally reduced temperatures lead to dryness and compromised skin barrier functions.<sup>3,4,13,15-17</sup> Since the physical characteristic of thermal insulation of a skin-interfacing object is known to affect the localised skin temperatures at the interface site (hence the concept of thermal clothing), it is important to understand the relative extent of thermal insulation of any objects and materials that may potentially contact or be in close proximity to a patient's body. Among such objects and materials are clothing, garments and diapers, bedsheets, and also, very commonly, dressings.

Other than treatment dressings, prophylactic PU dressings are gaining popularity as part of PU prevention strategies. The biomechanical protective effects of both types of dressings have been studied extensively in recent years,

primarily by our group,<sup>18-26</sup> and our findings were supported by several large-scale randomised clinical trials (RCTs).<sup>27-29</sup> With that said, all dressings induce some physical occlusion to skin, and, therefore, all dressings may potentially interfere under the neutral skin microclimate conditions, as heat could be accumulated between a dressing and the covered skin. Changes in skin temperature and moisture are nearly inevitable in seriously ill patients and in real-world clinical environments, and such conditions should be managed to the best possible extent to protect tissues. Although the concept of microclimate and its effects on PU risks and deterioration of existing wounds are increasingly gaining attention from clinicians and researchers, knowledge concerning heat accumulation under dressings is relatively poor. We conducted a PubMed and Google Scholar database search using the terms “microclimate,” “skin,” “temperature,” and “dressing” that yielded four papers, which quantitatively addressed the issue of microclimate under dressings: a paper by Call and colleagues<sup>30</sup> where they utilised a physical phantom, two additional papers that report skin temperatures under dressings applied to intact skin<sup>31</sup> and to wounds,<sup>32</sup> and our own recent work reporting preliminary results of an infrared thermography (IRT) study.<sup>17</sup> The general goal of this study was to investigate the effects of dressings on the microclimate of buttocks skin, while a patient is lying in a weight-bearing supine position, and, to determine the combined influence of the mechanical and thermal properties of dressings on skin microclimate under and near the dressings. Using the presently developed bioengineering methodology, we specifically aimed to quantitatively compare skin temperatures and heat accumulation under a polymeric membrane dressing (PMD; PolyMem, Ferris Mfg. Corp., Fort Worth, TX) with those under a standard placebo foam dressing. We describe here the detailed integrated experimental-computational work for the above purpose, including laboratory measurements of mechanical and thermal material properties of the aforementioned dressings, conducted to inform a three-dimensional anatomically realistic multiphysics finite element (FE) model, originally developed by our group. The role of FE modelling in the study of dressings and the vast progress that we have achieved in the field in the last several years has been described in our recent comprehensive review article,<sup>26</sup> and interested readers are referred to this published work for detailed explanations concerning the necessity in using FE modelling to establish efficacy of dressings.

The present study is a direct continuation of our earlier published work where we have developed a theoretical framework to study heat accumulation between patient bodies and support surfaces.<sup>33</sup> Here, for the first time in the literature, we have added the fundamentally

important aspect of the impact of dressings (as an interface layer in-between the skin and support) on skin microclimate. Accordingly, this article highlights how thermal properties of dressings, thermal conductivity in particular, are important in effectively mitigating the risk of developing a new PU or aggravation of an existing one.

## 2 | METHODS

To determine the effects of dressings on the microclimate of buttocks skin while a patient is lying in a weight-bearing supine position, we first characterised the density, stiffness, and thermal conductivity properties of two types of dressings: (i) a PMD (PolyMem, Ferris Mfg. Corp., Fort Worth, TX) and (ii) a standard semipermeable polyurethane dressing, which is referred to here as “placebo foam dressing.” This latter foam dressing had specimen dimensions that were equal to those of the PMD, but it was lacking the specific active PMD components, which act synergistically to result in inflammation modulation in skin and deep tissues wherever applied.<sup>1,34</sup> We then developed a multiphysics three-dimensional (3D) anatomically realistic FE model of the buttocks in which each cheek of the buttocks has been covered by one of the aforementioned two dressings. An additional FE model variant of bare buttocks was developed to assess the impact of each type of dressing relative to the case in which no dressing is used. In both model variants, the buttocks have been laid on a standard medical foam mattress. We specifically aimed to compare skin temperature magnitudes and distributions between the cases with and without dressings and for each dressing type. These systematic comparisons enabled objective, standardised, and quantitative evaluations of the influence of the material characteristics and engineering design features of dressings on skin microclimate.

### 2.1 | Engineering characterisation of dressing materials

#### 2.1.1 | Density and stiffness measurements in dry conditions

The apparent density of the dry dressing materials was determined by measuring the volume and weight of three  $5 \times 5 \text{ cm}^2$  test specimens for each dressing sample. The dimensions and weights were measured using a Vernier calliper with resolution of 0.05 mm and a GF-2000 precision balance (A&D Ltd., Tokyo, Japan), respectively. Average apparent density values were then calculated as volume/weight ratio (per measurement set). Stiffness

properties of dressings in dry conditions were further measured at ambient conditions of  $23 \pm 1^\circ\text{C}$  and relative humidity of 50% using an electromechanical testing machine (Instron model 5944, Norwood MA) according to the ASTM 3574 uniaxial compression testing standard. A load cell with a capacity of 2 kN and precision of 1/1000 of that load cell capacity has been employed, and the deformation rate has been set as  $50 \pm 5$  mm/min. The elastic moduli of three test specimens of each dressing material were calculated as the mean slope of the stress–strain curve obtained in each test for a strain domain of 10% to 40%.

### 2.1.2 | Thermal conductivity studies

To determine the thermal conductivity of the dry dressing materials, a custom-made testing device was assembled, as follows (Figure 1). Dressing specimens, cut to the approximate size of  $4 \times 4$  cm<sup>2</sup> and thickness of 2–3 mm, were placed between brass and aluminium blocks, each with a size of  $37 \times 37 \times 50$  mm<sup>3</sup>. Thermocouples were soldered at equal distances along these brass and aluminium blocks, and temperature readings from each were digitally and automatically recorded using the LabView data acquisition software (Version 7.2, National Instruments, Austin, TX).<sup>35</sup> An electrical silicon heating mat (RS Components Ltd., Corby, UK) placed on top of the brass block transferred heat flux, which was controlled using a power supplier (Techno Instruments (Pvt) Ltd., Kalubowila, Sri Lanka). An inferior cooling plate, located underneath the aluminium block, was cooled using a water flow system to create a relatively large temperature gradient over the smaller (test chamber) distance in the testing device. The silicon heating mat, brass block,

dressing specimen, and aluminium block compartments were all isolated to impose a (theoretically) unidirectional heat flux through the system, perpendicular to the dressing sample, that is, so that the heat flux is transferred along the thickness axis of the dressing. The ambient conditions at the room were  $23 \pm 1^\circ\text{C}$  and relative humidity of 50%. We applied pressure of 3.4 kPa on the samples using precision weights. Temperature readings were collected for four preadjusted equal intervals of heat flux. We waited for 15 minutes to reach steady-state heat distributions after each time where the heat flux has been raised by increasing the voltage generated through the power supplier. After each such waiting time interval, readings from the temperature sensors were stable. For each heat flux level, five readings were taken from all thermocouples at time intervals of 30 seconds. The five temperature values measured by each thermocouple were then averaged, and the thermal conductivity was calculated for each heat flux level.

Specifically, the thermal conductivity coefficient  $K$  of the dressing materials ( $K_{\text{dressing}}$ ) was calculated using Fourier's law for 1D heat transfer under the assumption that the heat flux along the brass, dressing, and aluminium materials was equal in the experiments due to the complete thermal isolation of the testing device from the environment:

$$Q = K_{\text{brass}} \cdot A \cdot \frac{T_1 - T_{2A}}{X_{\text{brass}}} = K_{\text{dressing}} \cdot A \cdot \frac{T_{2A} - T_{2B}}{t} = K_{\text{aluminium}} \cdot A \cdot \frac{T_{2B} - T_3}{X_{\text{aluminium}}}, \quad (1)$$

where  $Q$  (W/m<sup>2</sup>) is the heat flux,  $A$  (m<sup>2</sup>) is the contact area of the samples, and  $T_{2A}$  (°C) and  $T_{2B}$  (°C) are the measured temperatures at the superior and inferior borders of the dressing specimen, respectively (calculated from the temperature gradients in the brass and aluminium blocks). The temperature  $T_1$  (°C) is that of the highest thermocouple in the brass block, and  $T_3$  (°C) is the temperature at the lowest thermocouple in the aluminium block. The thickness of the tested dressing specimen is  $t$  (m), and  $X$  (m) is the length of the block.  $K_{\text{brass}}$  (W/mK) and  $K_{\text{aluminium}}$  (W/mK) are the thermal conductivity of the brass and aluminium blocks, respectively. Reordering terms and isolating the parameter of interest,  $K_{\text{dressing}}$  (W/mK), yields

$$K_{\text{dressing}} = \frac{K_{\text{brass}}}{X_{\text{brass}}} \cdot t \cdot \frac{T_1 - T_{2A}}{T_{2A} - T_{2B}}. \quad (2)$$

### 2.1.3 | Statistical analyses of empirical data

We report descriptive statistics of average  $\pm$  SD for all measurements. Unpaired, two-tailed  $t$  tests were

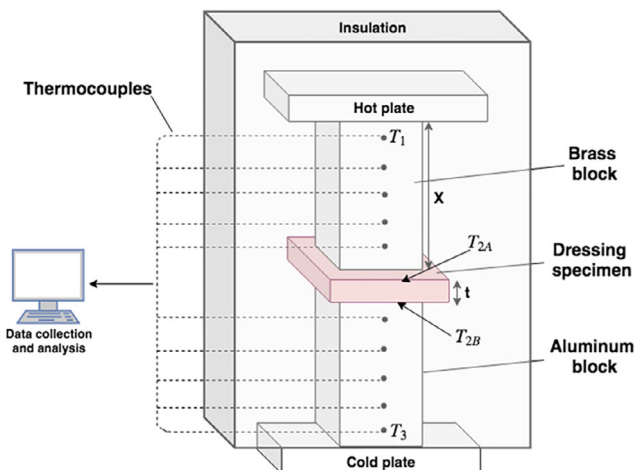


**FIGURE 1** Schematic diagram of the thermal conductivity testing device



conducted to compare between the PMD and placebo properties per each measured parameter. Statistical significance was considered for  $P < .05$ .

### 2.1.4 | Geometry of the computational model

The 3D model of the buttocks was developed using 76 T1-weighted axial magnetic resonance imaging (MRI) slices of the weight-bearing buttocks of a 28-year-old healthy female subject. The slices were imported to the ScanIP module of the Simpleware software (Synopsis Co., Mountain View, CA) for segmentation of the bones, skeletal muscles, fat and skin tissues (Figure 2A). The two dressing types, each with approximate area of  $10 \times 10 \text{ cm}^2$  and thickness of 3 mm, were placed nearly symmetrical on each cheek of the buttocks at the sites of the ischial tuberosities. A flat foam mattress was further added under the buttocks (Figure 2B).

## 2.2 | Numerical method

Meshing of the tissues, two dressings and mattress components, was performed using the ScanIP module of Simpleware.<sup>36</sup> Four-node thermally coupled tetrahedron elements (C3D4T) were used in all model components. Mesh refinements were applied locally in skin-mattress and dressing-mattress interfaces to reach adequate convergence of the numerical solution. There were a total of more than 1.5 million elements in the FE model variant with the dressings, with the following breakdown: 164 105 mattress elements, 183 484 skin elements, 431 616 fat elements, 532 587 skeletal muscle elements, 210 536 bone tissue elements, and 65 565 dressing elements (Figure 2C). The meshed geometry was then imported to the ABAQUS CAE 2017 Standard Solver (Dassault Systems, Vélizy-Villacoublay, France) for the set-up of the coupled structural-thermal analysis.<sup>37</sup> Converging time steps were chosen for the numerical data collection, so that the resulting bodyweight reaction force deviated from the target

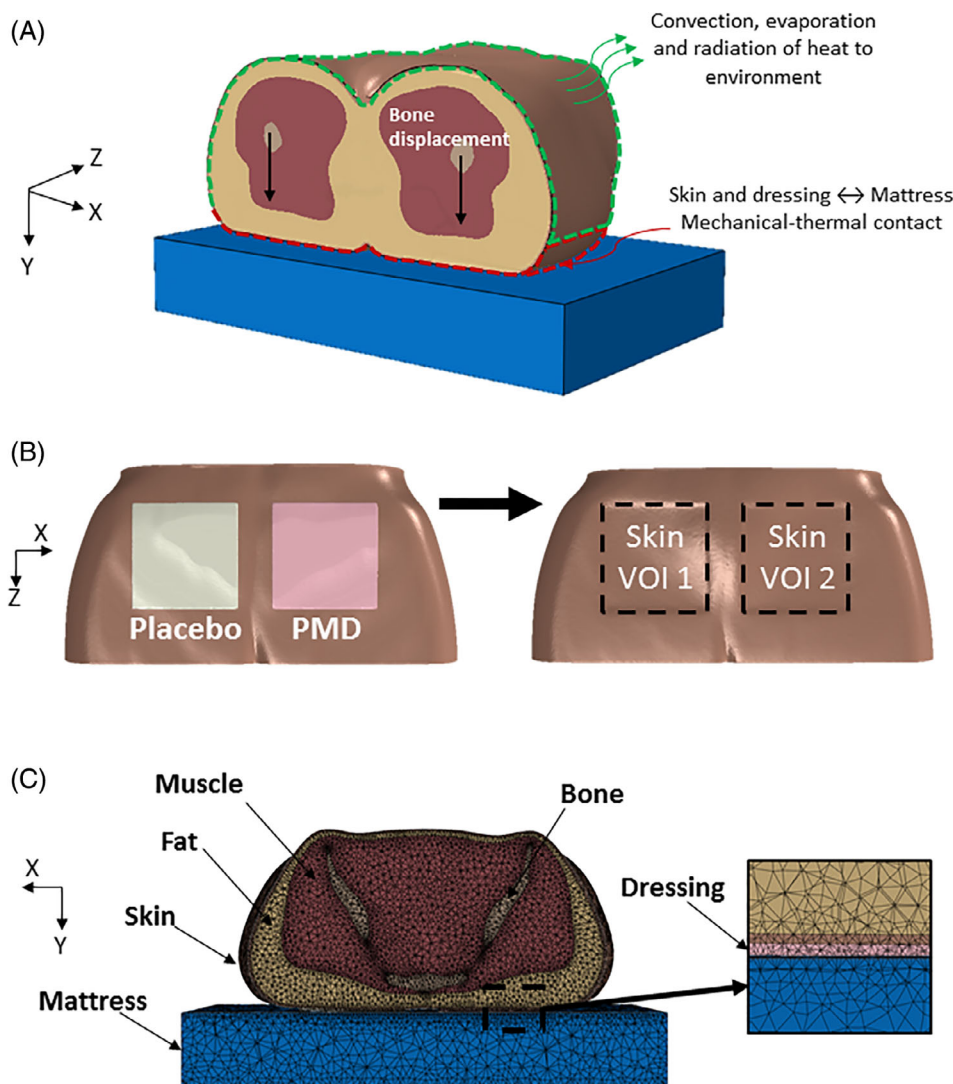


**FIGURE 2** Finite element computational modelling of the buttocks with a polymeric membrane dressing (PMD, PolyMem; Ferris Mfg. Corp., Fort Worth, TX) and matched placebo dressing (lacking the inflammation modulating components of the PMD) on the right and left sides of the buttocks, respectively. A, The applied mechanical and thermal loading and boundary conditions. B, geometric model of the skin and dressings (left); definition of the boundaries of the two volumes of interest of skin under the two dressings (right). C, The tetrahedral mesh of the pelvic region, the PMD, and placebo dressings and the mattress in an axial cross section

**TABLE 1** Mechanical properties of the tissues, dressings (PMD = polymeric membrane dressing), and mattress

Model component	Neo-Hookean material parameter $C_{10}$ (kPa)	Initial bulk modulus $K_0$ (kPa)	Poisson's ratio $\nu$	Elastic modulus $E$ (kPa)
Skin <sup>a</sup>	4	666.67	0.494	-
Fat <sup>a</sup>	0.4	66.67	0.494	-
Skeletal muscle <sup>a</sup>	0.225	37.5	0.494	-
Bone <sup>b</sup>	-	-	0.3	$7 \times 10^6$
Mattress <sup>c</sup>	-	-	0.3	7.5
PMD <sup>d</sup>	-	-	0.3	15.5
Placebo <sup>d</sup>	-	-	0.3	33.5

<sup>a</sup>Zeevi et al.<sup>33</sup><sup>b</sup>Linder-Ganz et al, Palevski et al, and Gefen et al.<sup>38-40</sup><sup>c</sup>Peko Cohen et al.<sup>41</sup><sup>d</sup>Experimental results described in detail in Section 3.1.

reaction force by no more than 0.8%. The time for solving each simulation case, using a 64-bit Windows 10-based workstation with Intel Core i9-7900X 3.30 GHz CPU and 64 GB of RAM, was approximately 65 hours. In other words, due to the complex structural-thermal coupling in this novel modelling framework, each FE simulation required nearly 3 days to run up to completion on the abovementioned powerful workstation.

### 2.3 | Biomechanical model and mechanical properties

Constitutive laws and mechanical properties of the tissue components and the mattress were adopted from the literature. Specifically, bone tissues (sacrum and femurs) were modelled as a linear-elastic isotropic material with an elastic modulus of 7 GPa and a Poisson ratio of 0.3.<sup>38-40</sup> Muscle, fat, and skin tissues were assumed to behave as homogeneous-isotropic-hyperelastic materials that follow a large strain elasticity behaviour through the neo-Hookean form of strain energy density potential, with a strain energy density function  $W$ :

$$W = C_{10}(\bar{I}_1 - 3) + \frac{1}{D_1}(J_{el} - 1), \quad (3)$$

where  $\bar{I}_1$  is the first invariant of the right Cauchy-Green deformation tensor,  $C_{10}$  [kPa] is a material stiffness parameter,  $J_{el}$  is the determinant of the deformation gradient tensor, and  $D_1$  is

$$D_1 = \frac{2}{K_0}, \quad (4)$$

where  $K_0$  (kPa) is the initial bulk modulus of the material. The material constants that were used here were

obtained in earlier work of our group<sup>33</sup> (Table 1). The mattress was considered linear-elastic isotropic material with an elastic modulus of 7.5 kPa and a Poisson ratio of 0.3, again, based on the literature.<sup>41</sup> The mechanical properties of the dressing materials were determined experimentally as described in Section 2.1, and the results for these studies are reported in Section 3.1 and Table 1.

### 2.4 | Biothermal model and thermal properties

The passive and active thermoregulation systems of the body were represented using the Fiala's thermoregulation modelling framework.<sup>42,43</sup> The fundamental heat transfer balance within biological tissues was formulated by means of the Pennes equation<sup>44</sup>:

$$k\nabla^2 T + q_m + \rho_{bl} w_{bl} c_{bl} (T_{bl,a} - T) = \rho c \frac{\partial T}{\partial t}, \quad (5)$$

where  $k$  (W/mK) is the thermal conductivity of the tissue of interest,  $T$  (°C) is the temperature of that tissue,  $q_m$  (W/m<sup>3</sup>) is the metabolic heat rate of the same tissue;  $q_{bl}$  (kg/m<sup>3</sup>),  $w_{bl}$  (s<sup>-1</sup>), and  $c_{bl}$  (J/kg K) are the blood density, perfusion rate, and heat capacity, respectively; and  $T_{bl, a}$  (°C) is the arterial blood temperature. The rate of temperature change over time  $\partial T / \partial t$  (°C/s) is considered to be zero since a steady state has been assumed. Under neutrality conditions, the heat rate and perfusion rate of a given tissue are set to be at basal levels, and as the tissue temperature begins to differ from its natural state, their values are changed as a function of that forming temperature difference. The equations for calculating the updated  $q_m$  and  $w_b$  considering the current tissue temperature were also adopted from Fiala's passive model<sup>42</sup>:

**TABLE 2** Thermal properties of the tissues, dressings (PMD = polymeric membrane dressing), and mattress

Model component	Thermal conductivity $k$ (W/mK)	Specific heat $C_p$ (J/kg K)	Density $\rho$ (kg/m <sup>3</sup> )	Basal metabolic rate $q_{m,0}$ (W/m <sup>3</sup> )	Basal blood perfusion $w_{bl,0}$ (s <sup>-1</sup> )
Skin <sup>a</sup>	0.47	3680	1085	368	$1.05 \times 10^{-3}$
Fat <sup>a</sup>	0.16	2300	850	58	$3.60 \times 10^{-6}$
Skeletal muscle <sup>a</sup>	0.42	3768	1085	684	$5.38 \times 10^{-4}$
Bone <sup>a</sup>	0.75	1700	1357	0	0
Mattress <sup>b,c</sup>	0.026	1000	40	-	-
PMD <sup>d</sup>	0.089	1000	210	-	-
Placebo <sup>d</sup>	0.058	1000	227	-	-

<sup>a</sup>Fiala et al.<sup>45</sup><sup>b</sup>Prasad et al.<sup>46</sup><sup>c</sup>Jarflat et al.<sup>47</sup><sup>d</sup>Experimental results described in detail in Section 3.1.

$$q_m = q_{m,0} + \Delta q_m, \quad (6)$$

where  $\Delta q_m$  (W/m<sup>3</sup>) is considered here as the additional heat rate due to possible local autonomic thermoregulation, neglecting the possible metabolism due to shivering and exercising (which are irrelevant in the pressure ulcer research context). The  $\Delta q_m$  value is hence calculated according to the following equation:

$$\Delta q_m = q_{m,0} \cdot \left[ 2^{\frac{T-T_0}{10}} - 1 \right], \quad (7)$$

where  $T_0$  (°C) is the tissue temperature at its set point. The blood perfusion rate varies with potential changes in local metabolic heat rate:

$$w_{bl} = w_{bl,0} + \Delta w_{bl}, \quad (8)$$

where  $w_{bl,0}$  (s<sup>-1</sup>) is the basal blood perfusion rate and  $\Delta w_{bl}$  (s<sup>-1</sup>) is the change in demand for oxygen as a function of the change in metabolic rate:

$$w_{bl} = w_{bl,0} + \frac{\mu_{bl} \cdot \Delta q_m}{\rho_{bl} c_{bl}}, \quad (9)$$

where  $\mu_{bl}$  is the proportionality constant. The passive blood circulation was assumed to be in equilibrium, that is, the blood pool temperature was assumed to be equal to the venous temperature, and the counter-current heat exchange between blood vessels was not incorporated into the present modelling; hence,  $T_{bl,a}$  is constant. A volumetric heat production by the muscle, fat, and skin tissues was calculated according to the thermal model, which was described earlier, using a specially developed HETVAL Fortran subroutine that was implemented in the computational model and integrated in the ABAQUS

simulation codes. The thermal properties of the tissues and mattress were adopted from the literature.<sup>45-47</sup> The thermal properties of the dressings were measured in our present work (as described earlier) and the results are specified in Section 3.1 (Table 2).

## 2.5 | Boundary conditions and loads

To investigate the coupled biomechanical-biothermal behaviour of the soft tissues of the buttocks during supine bedrest, in interaction with the studied dressings, which are attached to the noninjured buttocks as in prophylactic use, we applied bodyweight forces to the modelling. Specifically, we sought to simulate the descent of the weight-bearing pelvic and sacral bones, together with the heat transfer between the body and the environment (including the dressings and mattress). For this purpose, a downward displacement of 2.1 cm (in the Y-direction of the model) was applied on the bones (Figure 2A). The bottom of the mattress was fixed for all motions so that only the buttocks tissues and attached dressings were able to move, whereas the mattress was able to deform under the bodyweight forces but not to perform a “free-body-motion.” These virtual loading conditions mimic reality, where a mattress is placed on a bedframe. Surface-to-surface frictional contact was further defined between the skin and dressing surfaces and the superior surface of the mattress; the COF at these contact sites was set as 0.4.<sup>22,48</sup>

The thermal model was first solved separately in a steady-state heat transfer simulation to obtain the temperature field in the buttocks under the following thermal neutrality conditions: ambient temperature  $T_{amb}$  of 28°C, air velocity  $v_{air}$  of 0.05 m/s, relative humidity RH of 40%, and surrounding wall emissivity  $\epsilon_w$  of 0.93.

Heat transfer by radiation was calculated according to Fiala's thermoregulation modelling framework by Fiala et al.<sup>42</sup>:

$$q_R = h_R \cdot (T_{sk} - T_{amb}), \quad (10)$$

where  $T_{sk} = 33.5^\circ \text{C}$  is the area-weighted mean skin temperature,  $T_{amb} = 28^\circ \text{C}$  is the ambient temperature, and  $h_R$  is calculated by

$$h_r = \sigma \epsilon_{sf} \epsilon_{sr} \psi_{sf-sr} \cdot (T_{sk}^{*2} + T_{amb}^{*2}) (T_{sk}^* + T_{amb}^*), \quad (11)$$

where  $\sigma = 5.67 \cdot 10^{-8} \text{ (W/m}^2\text{K}^4\text{)}$  is the Boltzmann constant,  $\epsilon_{sf} = 0.99$  and  $\epsilon_{sr} = 0.93$  are the emission coefficients of the body and of the surrounding surfaces, respectively,  $\psi_{sf-sr} = 0.9$  is the corresponding view factor,  $T_{sk}^*$  and  $T_{amb}^*$  ( $^\circ\text{C}$ ) are the absolute temperatures of the local skin sector and of the surrounding surfaces, respectively. Heat fluxes by convection, radiation, and evaporation from the body to the environment were set between the whole skin surface in the model and the surroundings, and calculated using the Fortran FILM and DFLUX subroutines, which were integrated in the ABAQUS simulation codes. This solution was used as initial conditions for the buttocks temperature in the full structural-thermal coupled modelling. The initial temperatures of the mattress and dressings were considered to be uniform and set as  $28^\circ\text{C}$ .

In the structural-thermal coupled model, the skin surface was divided into two regions of interest (ROIs). The first region included skin elements in the rear side of the buttocks, which are at an initial distance of 3 cm or less from the superior surface of the mattress. The second region included the rest of the skin elements, which do not come into contact with the mattress during the simulations (Figure 2A). For the first ROI, we assumed heat transfer through thermal conductance only between the body and mattress. We used the Fortran GAPCON subroutine, which has been integrated in the ABAQUS simulation codes to calculate the conductance in the gap between the inferior skin surface and the top mattress surface, as a function of the distance between them. For the second ROI, we assumed heat transfer by convection, radiation, and evaporation to the environment. In that context, the skin stiffness material parameter  $C_{10}$  was defined as a function of the skin temperature, according to the findings of Patel and colleagues.<sup>49</sup> Specifically, they have found that as the skin temperature increases from  $28^\circ\text{C}$  to  $36^\circ\text{C}$ , the respective skin stiffness increases by 25%, which is approximately more than 3% greater stiffness per each  $1^\circ\text{C}$  increment.

A total reaction force of 56 N has been obtained for the studied buttocks segment (Figure 2A) for all model variants. This represents approximately 11% of the total bodyweight force of the subject, which is applied locally at the pelvic region.

## 2.6 | Outcome measures from the computational structural-thermal modelling

The outcome measures listed in the following were obtained for the modelling framework and boundary conditions that have been described earlier, which were identical for both the model variant with dressings and the variant without the dressings. The left and right sides of the buttocks in the modelling were not precisely symmetrical due to the realistic subject anatomy that has been captured by means of the MRI scan. Accordingly, we compared the dressing types by examining the differences between the cases with vs without dressing per each side (cheek) of the buttocks (right side with the PMD, and left with the placebo). We specifically defined two cubical volumes of interest (VOIs) in the buttocks tissues, each included the elements of skin directly under the dressing, and then, we have systematically compared temperature magnitudes and distribution in each VOI between the cases with vs without a dressing (Figure 2B). The volumetric exposures of skin to elevated temperatures were analysed for the two VOIs, using temperature exposure histogram (TEH) charts, as per a similar methodology developed in our previous work for structural loads in tissues.<sup>20,21</sup> As a final step in the computational analyses, we determined a protective heat clearance index (PHCI) of the two dressing types by calculating the relative % differences in the area under the TEH curves, separately for the PMD and placebo dressing, relative to the case where no dressing has been applied (bare buttocks):

$$\text{PHCI}[\%] = \frac{S_{\text{No dressing}} - S_{\text{Dressing}}}{S_{\text{No dressing}}} \cdot 100, \quad (12)$$

where  $S$  is the area under the TEH curve of each case.

## 2.7 | Experimental validation

The computational results of the heat transfer simulations, which were used here to obtain the thermal neutrality conditions of the body tissues, and the additional results of the full coupled structural-thermal simulations, were validated against empirical skin temperature measurements acquired by means of high-resolution IRT



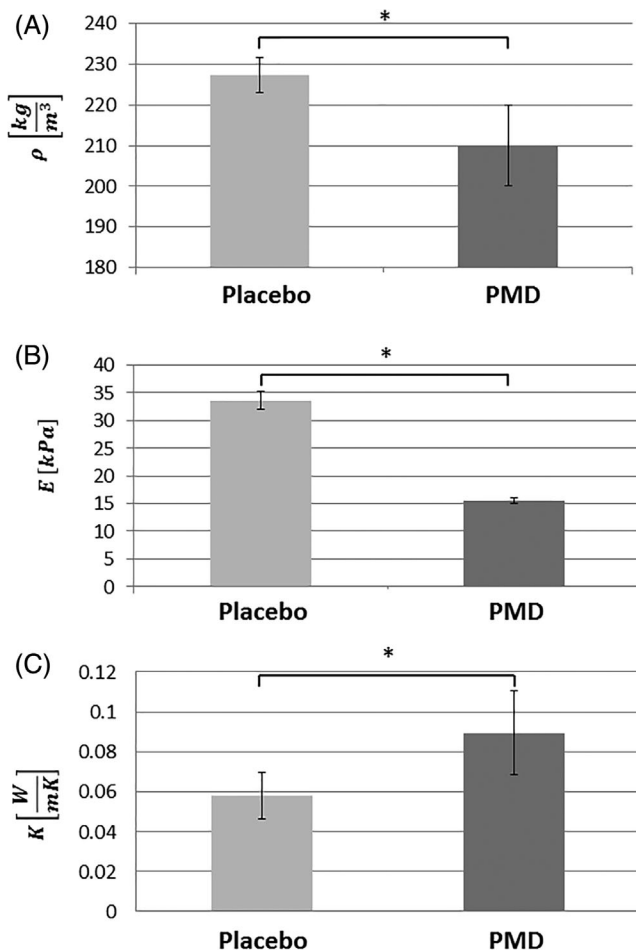


**FIGURE 3** Engineering characterisation of the dressing materials. A, Apparent density; B, stiffness; C, thermal conductivity. PMD, polymeric membrane dressing (PolyMem, Ferris Mfg. Corp., Fort Worth, TX). Placebo = matched foam dressing (lacking the inflammation modulating components of the PMD). Error bars are the SD from the mean ( $N = 4$  specimens per each dressing and trial type). \* $P < .05$

imaging. Our IRT experimental work to characterise the microclimate of skin tissues under dressings has been recently reported by Gefen et al<sup>17</sup> and is briefly described here for completeness. After acquiring baseline steady-state temperature images of the two buttocks sides in three healthy adult subjects (age range: 25–31 years, height: 159–164 cm, weight 43–65 kg) who were lying prone (ie, so that the buttocks tissues were not weight bearing), PMD and placebo dressings of the sizes used in the present FE modelling were attached to their right and left buttock cheeks, respectively, as described earlier for the present modelling work (Figure 2B). The IRT temperature measurements were then repeated following nearly motionless lying for 1 hour in a Fowler's position, immediately after removing both dressings. The average skin temperatures measured by means of IRT in the body regions similar to the ones considered in the

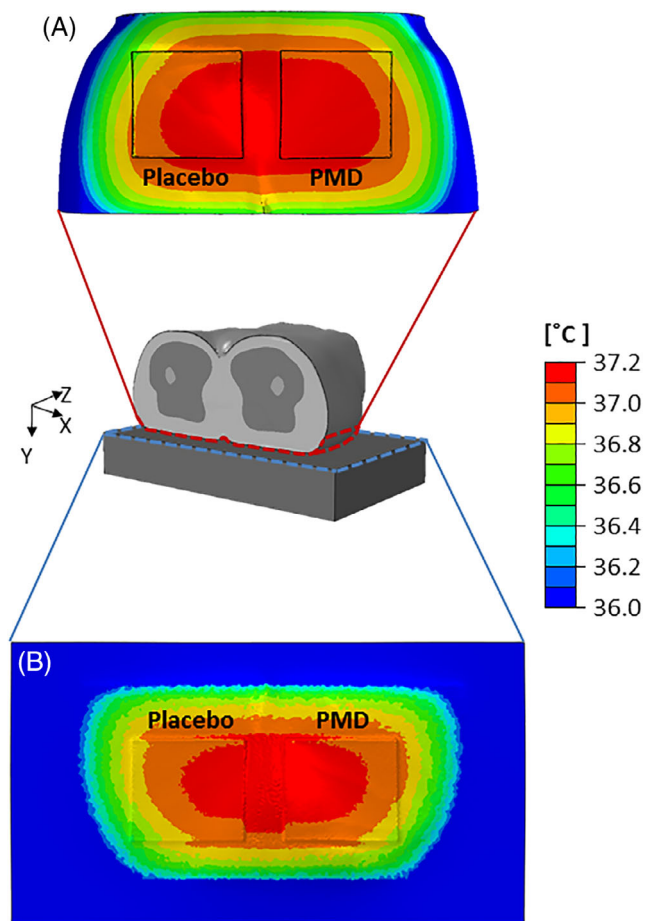


**FIGURE 4** The temperature distributions resulting from the weight-bearing supine lying simulations on the (A) dressings and surrounding skin and (B) superior surface of the mattress. The heat transferred from the tissues through the dressings and on to the mattress during weight-bearing conditions resulted in lower temperatures of the placebo dressing itself (left frames) and the mattress underneath, compared with the polymeric membrane dressing (PMD, PolyMem, Ferris Mfg. Corp., Fort Worth, TX; right frames), which indicates more heat accumulation under the placebo dressing, at the skin-placebo dressing interface. It is worth noting that the PMD dressing mildly warms up given its superior thermal conductance, which clears heat away from the body through the dressing and hence reduces heat accumulation under the PMD dressing. Placebo = matched foam dressing (lacking the inflammation modulating components of the PMD)

computational model (Figure 2B) in basal conditions were  $33.9 \pm 1.9^\circ\text{C}$  and  $33.5 \pm 2^\circ\text{C}$  for the right and left buttocks sides, respectively. Immediately after the 1-hour supine lying session, these skin temperatures increased to  $36.6 \pm 1^\circ\text{C}$  and  $36.5 \pm 0.9^\circ\text{C}$  for the right and left buttocks sides, respectively. SDs of temperatures that were obtained are similar to those reported by Hayden and Cole,<sup>31</sup> who compared skin temperatures at the knees of patients who underwent knee arthroscopies and received PMD vs cotton gauze. Using a DermaTherm temperature

strip (incorporating liquid crystal technology for skin temperature measurements that requires contact with skin, and is therefore different from IRT), they obtained SDs of approximately  $1.7^{\circ}\text{C}$  which is similar to the SDs reported here.<sup>31</sup> These experimental data are also in excellent agreement with the present FE modelling results, as reported next.

### 3 | RESULTS

#### 3.1 | Engineering characterisation of dressing materials

##### 3.1.1 | Density and stiffness data

The average density of the placebo foam dressing material was  $227.4 \pm 4.3$  ( $\text{kg}/\text{m}^3$ ) and that of the PMD was  $210 \pm 9.8$  ( $\text{kg}/\text{m}^3$ ), that is, the placebo dressing was significantly 1.1 times denser than the PMD ( $P < .05$ ; Figure 3A). Consistently, and as foams are known to exhibit correlation between density and stiffness properties (typically a power law density-stiffness relationship exists), the elastic modulus of the placebo material was statistically significantly 2.1 times greater than that of the PMD (the average elastic modulus of the placebo dressing was  $33.5 \pm 1.6$  (kPa), whereas that of the PMD was  $15.5 \pm 0.4$  (kPa) ( $P < .05$ ; Figure 3B).

##### 3.1.2 | Thermal conductivity properties

The thermal conductivities of the placebo foam dressing and PMD were  $0.058 \pm 0.01$  (W/mK) and  $0.089 \pm 0.02$  (W/mK), respectively. The PMD is therefore a superior heat conductor with respect to the placebo, as it cleared heat energy away from the heat source 1.5 times statistically significantly more than the placebo ( $P < .05$ ; Figure 3C).<sup>1,34</sup>

#### 3.2 | Coupled structural-thermal computational model

In both FE model variants, metabolic heat generation in the soft tissues of the pelvic region resulted in heat transfer from the buttocks to the environment, as could be expected. Temperature distributions on the dressings and adjacent skin and on the superior surface of the mattress in the weight-bearing conditions are shown in Figure 4. The heat transferred from the body tissues through the dressings and on to the mattress by thermal conductance during weight-bearing conditions, which

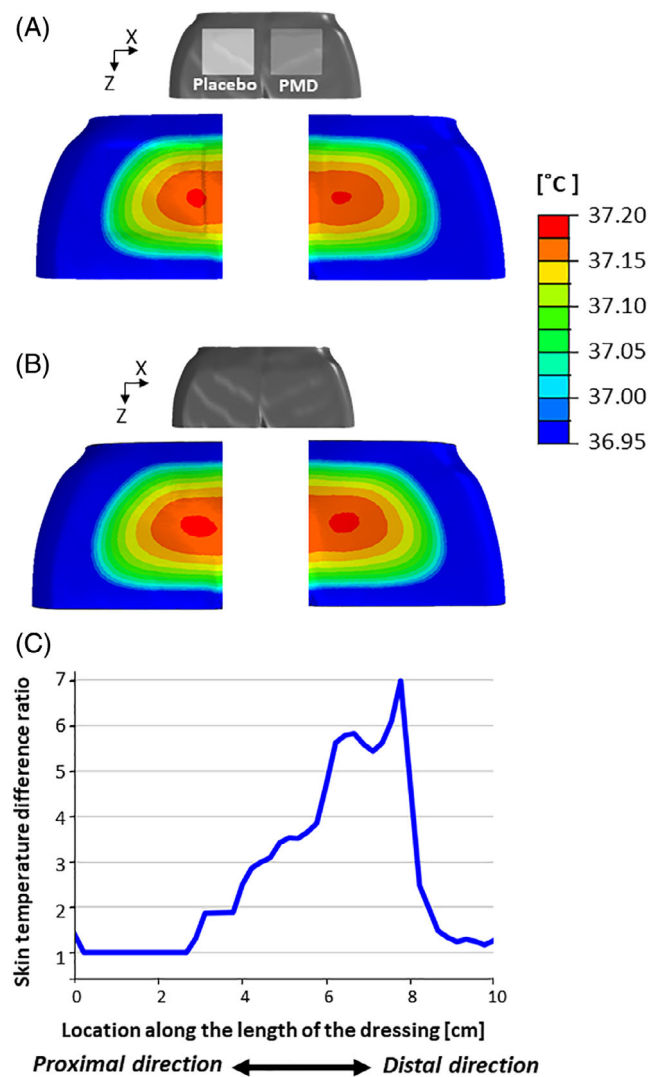


**FIGURE 5** Skin temperature distributions resulting from the weight-bearing supine lying simulations (A) under the placebo foam dressing (left buttocks side) and polymeric membrane dressing (PMD, PolyMem, Ferris Mfg. Corp., Fort Worth, TX at the right side) and (B) for the bare buttocks (both sides are without dressings). For both sides of the buttocks, skin temperatures were higher without dressings, as both dressing materials conduct heat better than the mattress (ie, there is less local heat accumulation on buttocks skin when applying a dressing compared to the bare buttocks state). The aforementioned observation may be counter-intuitive, but this depends on the specific thermal properties of the selected dressing and mattress. With that said, there has been greater temperature reduction in the case where the PMD was applied (right frames). C, The ratio between skin temperature differences obtained when the PMD was applied on the right buttock side, over the skin temperature differences obtained in the left buttock with the placebo dressing applied there, along a horizontal axis originated in the proximal side of each dressing

resulted in lower temperatures of the placebo dressing itself and the mattress underneath, compared with the PMD dressing, which indicates more heat accumulation

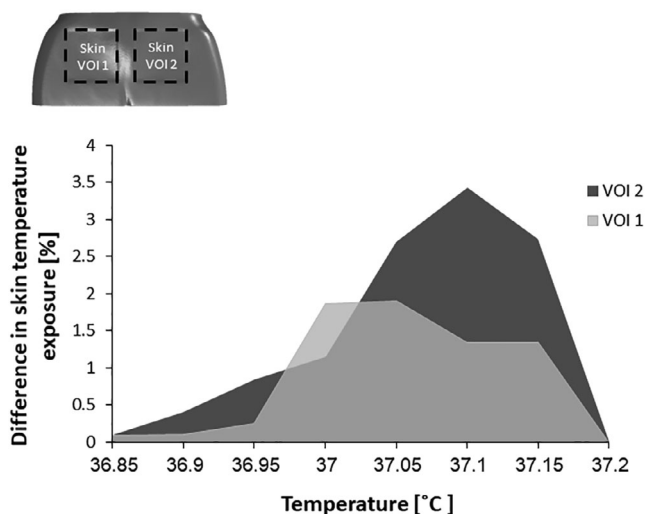


**FIGURE 6** Differences in skin cumulative temperature exposure between the no-dressing and dressing conditions, for each volume of interest (VOI) during weight bearing. A greater temperature difference indicates more heat conduction through the dressing and better clearance of potentially accumulated heat that may compromise skin integrity, properties, and function

under the placebo dressing, at the skin-placebo dressing interface (Figure 4). Contrarily, the PMD dressing mildly warms up given its better heat conductance, which clears heat away from the body tissues through the dressing and hence reduces heat accumulation under the dressing (Figure 4). Temperature distributions on skin during weight-bearing conditions at the left and right buttocks cheeks, with and without the dressings, are shown in Figure 5A,B. For both sides of the buttocks, skin temperatures were higher without dressings, and hence the average skin temperatures in the two VOIs were slightly reduced when dressings were used, as both dressing materials conduct heat better than the mattress so in general there is less local heat accumulation on the buttocks skin when applying a dressing compared to the bare buttocks state (which is counter-intuitive, but would depend on the specific thermal properties of the selected dressing and mattress). With that said, there has been greater temperature reduction in the right VOI where skin was in contact with the PMD. Specifically, the reduction of average skin temperature demonstrated in the right VOI was 1.6 times greater than the reduction in the left side VOI, which was covered by the placebo dressing, again due to the greater thermal conductivity of the PMD. In Figure 5C, we quantitatively display the ratio between skin temperature differences obtained when the PMD was applied on the right buttock side, over the skin temperature differences obtained in the left buttock with the placebo dressing applied there.

To quantify the abovementioned complex phenomena in a practical engineering format that will further facilitate future systematic comparisons and rating of microclimate performances of prophylactic dressings, we have used the percentage difference between the cumulative volumetric skin temperature exposure in the no-dressing case vs the respective case where a dressing has been applied. These data are depicted in Figure 6 for each of the two studied dressing types (VOIs). Consistent with all the experimental and computational findings reported earlier, the results shown in Figure 6 demonstrate considerable reduction in skin exposure to elevated temperatures when the PMD dressing is applied, compared to placebo, particularly as concerned the higher temperature range (which, in real-world conditions, could be associated with any potentially ongoing inflammatory process). This difference between the dressing performances is also evident and quantifiable by means of the PHCI values, being 3.4% for the PMD compared to just 2.4% for the placebo dressing, that is, the PHCI of PMD is 1.42 times greater than that of the placebo foam).

## 4 | DISCUSSION

In this study, we aimed to investigate the effects of dressings on the microclimate of buttocks skin in a patient lying in a weight-bearing supine position. The body-dressing-environment interactions were investigated in a prophylactic context here, but in future work, a similar computer modelling approach can be expanded to wound treatment as well. The biomechanical modes of action and function of prophylactic dressings in PU prevention and treatment were extensively studied, primarily by our group.<sup>18-26</sup> However, the thermal properties and performances of dressings and the effects of these thermal properties on body tissues, in the context of PU prevention, were evaluated here for the first time in the literature. We specifically focused on assessing skin temperatures directly under the dressings, and on experimentally and mathematically formulating the relevant heat transfer phenomena and body-dressing-environment thermal interactions. We specifically compared a PMD dressing, containing the complex composition of inflammation modulating components,<sup>1,34</sup> against a placebo standard foam dressing with the same shape and dimensions. We first performed rigorous laboratory tests to characterise the engineering properties of each dressing type, and the empirical results were then implemented in a multiphysics computational anatomically realistic FE model, which facilitated methodological quantitative comparisons between the structural-thermal effects of these two dressings on the body tissues.

Our present simulation data, based on *in vitro* and *in vivo* experimental work, confirmed that skin and subdermal tissue temperatures increase and that heat is naturally being accumulated at the contact areas between the buttocks and dressings or support surface. This is reasonable and well expected from both a physical perspective and a physiological perspective, because heat conductance from the core of the body to external surfaces should depend on the aforementioned contact areas, which in turn, relate to the bodyweight forces and their pattern of distribution. Moreover, our experimental-computational results, considered together, demonstrated that the engineering properties of the materials that are in contact with skin have a distinguished impact on the resulted skin temperature increase, and in particular, on the heat accumulation between the skin covered by the dressing and the contacting dressing in combination with the support surface in use. Specifically, the placebo dressing, which was experimentally found to have lower thermal conductivity (1.5 times), greater density (1.1 times), and higher stiffness (2.1 times) with respect to the PMD dressing (Figure 3), was also shown by the computational modelling to cause more heat accumulation under its structure (Figures 4 and 5). This is consistent with knowledge that in foam materials, better thermal conductivity is correlated with lower density and stiffness.<sup>50</sup>

Since the thermal conductivity of the mattress in the present model is lower than those of the two tested dressing types, the insulation provided by the mattress is indeed greater where no dressings are present and the skin contacts the mattress directly. The thermal conductivity of the support surface is therefore critical as well and plays a major role in these complex body-object thermal interactions. These results are in agreement with our previously published work, focusing on support surfaces, where we reported that body tissues at the sacral area reached different temperatures, depending on the nature of the support surface.<sup>33</sup>

Temperature differences reported here between the dressing and no-dressing cases, and between the placebo and PMD dressings appear to be mild; however, they are physiologically and clinically meaningful in the context of computational modelling of intra-subject body temperatures. For example, Bhargava and colleagues reported that in the context of pressure ulcer prevention, the increase of intra-subject temperature between 0.25°C and 0.9°C could be associated with inflammation processes, whereas the decrease of intra-subject temperature between -0.2°C and -0.5°C could be associated with local ischaemia, that is, in both cases—of inflammation and ischaemia—the intra-subject temperature differences are within a fraction of 1°C.<sup>51</sup> Considering that the computational modelling framework used here is a

deterministic system, consistent differences in the microclimate conditions under the two dressing types (Figure 5C), despite being in the range of a fraction of 1°C, are meaningful, as they do not incorporate the variability that is characteristic to living model systems. The present article, together with that previously published work,<sup>33</sup> formulate the complete bioengineering theory to scientifically describe microclimate conditions in PU prevention research and development endeavours. The present approach can also be expanded to studies of skin microclimate in the context of management of diabetic foot ulcers, venous ulcers, surgical and traumatic wounds, and other chronic and acute wounds where dressings are being used.

During prolonged, stationary lying in bed or sitting, when bodyweight forces apply, an increase in local skin temperature at weight-bearing sites may have devastating consequences on skin and subdermal tissues, and would affect biological function and tissue metabolism rapidly, thus considerably contributing to the risk for new PUs. According to Patel and colleagues, a 1°C increase in skin temperature results in approximately 10% increase in metabolic demand.<sup>49</sup> Blood perfusion will increase in an attempt to meet these elevated metabolic demands of the affected tissues, consequently making these tissues more susceptible to ischaemic damage at lower deformation levels.<sup>3,52,53</sup> The Patel's study also reported that an increase in skin temperature results in skin stiffening, which promotes more mechanical stress concentrations in skin and underlying tissues as skin is locally less able to redistribute loads through (low level but widespread) deformations.<sup>14,49</sup> Furthermore, when skin temperatures increase over a threshold of approximately 33°C (depending on the core body temperature), local perspiration is triggered, which results in moisture on skin. That moisture softens the skin, leading to potential skin maceration and breakdown.<sup>53</sup> It is worth noting that the studies cited earlier is that Kokate and colleagues reported that for pressures above 100 mmHg, the severity, extent, and depth of tissue injury were closely related to the imposed temperature (in the 25°C-45°C range).<sup>54</sup> Taken together, the abovementioned literature indicates that minimising heat accumulation between the body and a dressing, or a support surface, or both, should be a priority for achieving effective PU prevention. It is also highly important to analyse the thermal conductivity of prevention dressing materials, as demonstrated here.

In this article, we introduced, for the first time in the wound care literature, an important index, the PHCI, which could be used to objectively and quantitatively assess the protective biothermal efficacy of dressings or dressing components. The PHCI reflects the ability of a dressing (or a dressing material) to clear body-generated



heat away from the contact area between the body and dressing, and, therefore, to prevent excessive heat accumulation. Hence, the greater the PHCI is, the better is the dressing (or dressing material) from a microclimate perspective. In the algorithm of calculation of the PHCI, dressing material properties and the thermal and mechanical loading scenarios are all taken into consideration, yielding a comprehensive evaluation of the preventative capacity of the dressing (material) under evaluation. Here, we found that the PHCI of the PMD dressing is 1.42 times greater than that of the placebo foam dressing. This means that more heat is likely to be accumulated under a simple foam dressing, leading to the localised increase of skin temperature and the negative consequences described earlier. Accordingly, material selection and composition in prophylactic dressings must account for the thermal conductivity of each component and the effective thermal conductivity of the composite. These, in addition to the mechanical (strength and stiffness) properties of the dressing components, are critical and will shape the nature of the tissue-dressing-environment interactions (including with regard to tissues' physiological and mechanical functions, integrity, and health). Ultimately, thermal conductivities of the dressing materials are a major factor determining the protective capacity of a dressing design/product.

Polymeric membrane dressings are hydrophilic and superabsorbent throughout their thickness. This is achieved via a complex composition of materials, one of which is glycerol (glycerine). The potential effect of glycerol on the thermal conductivity of PMDs should be considered as an example, while taking into account that there are additional materials (eg, surfactant) and interactions in the PMD products, which may influence their effective thermal characteristics. The beneficial effects of glycerol on skin have been well recognised, particularly for moisturising and smoothing in dermatological and cosmetic preparations. The diverse reported actions of glycerol on skin include improvement of SC hydration, skin barrier function and tissue mechanical properties, inhibition of the SC lipid-phase transition, protection against irritating stimuli, acceleration of wound healing and as an antimicrobial effect.<sup>55,56</sup> Glycerol is also known for its unique thermal characteristics, which facilitate its use as an antifreeze additive and cryoprotectant in medical cryopreservation. In the present context, it is likely that the role of glycerol in PMDs may extend beyond a therapeutic effect on skin to improve heat clearance through the dressing. This should be investigated further, including as related to febrile patients, burns, and other altered systemic or localised thermodynamic body and tissue conditions.

The clinical study of Hayden and Cole<sup>31</sup> is especially relevant to our current work as it reported that in a group of patients who underwent knee arthroscopy, following which a PMD was applied to the treated knee, skin temperatures at the knee region were statistically significantly lower (by approximately 1.5°C) under the PMD compared with those under cotton gauze dressings applied to a control group. The Hayden and Cole experimental findings<sup>31</sup> thereby agree with our present bioengineering analyses in demonstrating that PMDs provide better clearance of heat away from an inflamed tissue site, which minimises heat accumulation between the dressing and skin.

As with any modelling work, assumptions and limitations are inevitable and should be discussed here for completeness. The MRI anatomy used here is that of a healthy adult. Hence, the selected anatomy does not necessarily represent the wide variability in patient anatomies and conditions, or the risks of extreme body habitus conditions (such as obesity or cachexia). Likewise, the thermal model adopted from Fiala's work<sup>42,43,45</sup> does not consider acute/chronic diseases (persons prone to PUs are rarely healthy) or individual patient conditions such as hypothermia (eg, in unwarmed surgical patients) or hyperthermia (eg, in septic patients). With regard to the empirical skin temperature measurements, it is important to say that removal of the dressings in our experiments just prior to acquisition of IRT temperature maps of the skin could have promoted convective heat transfer from the skin to the environment; however, an alternative measurement method, using a thermocouple, would have only provided point measurement and would have had its own effects on measurement quality, including conduction of heat from the skin through the sensor and localised tissue deformations around the sensor under bodyweight loads. In addition, we did not consider the water vapour permeability and moisture absorption capacity of the tested dressings in our present computational modelling, although these are also relevant properties to characterise for objects in contact with skin. Additional extensive research and development of new Fortran/FE codes are needed to incorporate these complex physical phenomena in such multiphysics modelling. Moreover, to somewhat reduce the very high complexity of the present modelling framework, we assumed heat transfer by conduction only for the lower ROI (Figure 2A). Despite all these inherent limitations, our use of the same reference human anatomy, as well as measured biothermal and biomechanical properties of the body tissues in the modelling framework, facilitated the consistent, methodological, systematic, quantitative approach and comparisons that are reported here. Also of note is that the present approach is novel and pioneering



in the literature, and may be improved over time with advances in computer hardware, software, and FE modelling technology.

In conclusion, characterisation of the thermal properties and behaviour of prophylactic dressings was conducted here for the first time to determine their effects on skin and subdermal tissues in the primary context of PU prevention. Using an in silico approach based on relevant laboratory experiments and human validation studies, we identified heat conductivity of dressings and localised heat accumulation as highly important and relevant characteristics of dressing performances. We developed the experimental laboratory setups and procedures, protocols, and importantly, the biothermal theory and its mathematical formulation to obtain and describe the scientific evidence related to microclimate and PU care. This is as opposed to referring to “microclimate” in descriptive, qualitative terms, as often done in the literature. We specifically found here, using our novel approach and methodology, that the PMD dressing is able to reduce heat accumulation between the dressing and skin (relative to foam), which provides important protection to skin and subdermal tissues. The combination of structural biomechanical analyses of tissue deformations with concurrent evaluation of heat transfer in dressings/support surfaces and in tissues, as in our present multiphysics study, is highly innovative and points to the importance of material selection (particularly concerning thermal conductivity) in the design of dressings. Development of additional laboratory testing equipment and protocols and the corresponding computer modelling studies to evaluate heat conductivity of dressings and heat accumulation under dressings in scenarios simulating fever or hypothermia should be next steps in this bio-engineering research.

## ACKNOWLEDGEMENTS

This work was supported by an unrestricted educational grant from Ferris Mfg. Corp., Fort Worth, TX, USA.

## ORCID

Amit Gefen  <https://orcid.org/0000-0002-0223-7218>

## REFERENCES

- Gefen A. The future of pressure ulcer prevention is here: detecting and targeting inflammation early. *EWMA J* 2018; 19(2):7–13.
- Gefen A, Brienza D, Edsberg L, Milton W, Murphy C, Oomens CWJ, Perry L, Sari Y. The etiology of pressure injuries. In: *Prevention and Treatment of Pressure Ulcers/Injuries: Clinical Practice Guideline*. 3rd ed. European Pressure Ulcer Advisory Panel (EPUAP), National Pressure Injury Advisory Panel (NPIAP) and the Pan Pacific Pressure Injury Alliance (PPPIA); 2019.
- Kottner J, Black J, Call E, Gefen A, Santamaria N. Microclimate: a critical review in the context of pressure ulcer prevention. *Clin Biomech* 2018;59:62–70.
- Yusuf S, Okuwa M, Shigeta Y, Dai M, Iuchi T, Rahman S, Usman A, Kasim S, Sugama J, Nakatani T, Sanada H. Microclimate and development of pressure ulcers and superficial skin changes. *Int Wound J* 2015;12(1):40–46.
- Yoshimura M, Nakagami G, Iizaka S, et al. Microclimate is an independent risk factor for the development of intraoperatively acquired pressure ulcers in the park-bench position: a prospective observational study. *Wound Repair Regen* 2015;23(6):939–947.
- Geerligs M, Oomens C, Ackermans P, Baaijens F, Peters G. Linear shear response of the upper skin layers. *Biorheology* 2011;48:229–245.
- Takahashi M, Yamada M, Machida Y. a new method to evaluate the softening effect of cosmetic ingredients on the skin. *J Soc Cosmet Chem* 1984;35:171–181.
- Wilkes GL, Brown IA, Wildnauer RH. The biomechanical properties of skin. *CRC Crit Rev Bioeng* 1973;1:453–495.
- Sopher R, Gefen A. Effects of skin wrinkles, age and wetness on mechanical loads in the stratum corneum as related to skin lesions. *Med Biol Eng Comput* 2010;49(1):97–105.
- Egawa M, Oguri M, Kuwahara T, Takahashi M. Effect of exposure of human skin to a dry environment. *Skin Res Technol* 2002;8:212–218.
- Fluhr JW, Praessler J, Akengin A, Fuchs SM, Kleesz P, Grieshaber R, Elsner P. Air flow at different temperatures increases sodium lauryl sulphate-induced barrier disruption and irritation in vivo. *Br J Dermatol* 2005;152:1228–1234.
- Petrofsky J, Berk L, Alshammari F, et al. The interrelationship between air temperature and humidity as applied locally to the skin: the resultant response on skin temperature and blood flow with age differences. *Med Sci Monit* 2012;18(4):CR201–CR208.
- Engebretsen K, Johansen J, Kezic S, Linneberg A, Thyssen J. The effect of environmental humidity and temperature on skin barrier function and dermatitis. *J Eur Acad Dermatol Venereol* 2015;30(2):223–249.
- Atlas E, Yizhar Z, Khamis S, Slomka N, Hayek S, Gefen A. Utilization of the foot load monitor for evaluating deep plantar tissue stresses in patients with diabetes: proof-of-concept studies. *Gait Posture* 2009;29(3):377–382.
- Chen C, Hwang R, Chang S, Lu Y. Effects of temperature steps on human skin physiology and thermal sensation response. *Build Environ* 2011;46(11):2387–2397.
- Cravello B, Ferri A. Relationships between skin properties and environmental parameters. *Skin Res Technol* 2008;14(2):180–186.
- Gefen A, Peko Cohen L, Amrani G, Hoffer O, Ovadia-Blechman Z. The roles of infrared thermography in pressure ulcer research with focus on skin microclimate induced by medical devices and prophylactic dressings. *Wounds Int* 2019;10:8–15.
- Levy A, Gefen A. Assessment of the biomechanical effects of prophylactic sacral dressings on tissue loads: a computational modeling analysis. *Ostomy Wound Manag* 2017;63(10):48–55.
- Levy A, Schwartz D, Gefen A. The contribution of a directional preference of stiffness to the efficacy of prophylactic sacral dressings in protecting healthy and diabetic tissues from pressure injury: computational modelling studies. *Int Wound J* 2017;14(6):1370–1377.

20. Schwartz D, Levy A, Gefen A. A computer Modeling study to assess the durability of prophylactic dressings subjected to moisture in biomechanical pressure injury prevention. *Ostomy Wound Manag* 2018;64(7):18–26.
21. Schwartz D, Gefen A. The biomechanical protective effects of a treatment dressing on the soft tissues surrounding a non-offloaded sacral pressure ulcer. *Int Wound J* 2019;16(3):684–695.
22. Levy A, Frank BM, Gefen A. The biomechanical efficacy of dressings in preventing heel ulcers. *J Tissue Viability* 2015;24(1):1–11.
23. Levy A, Gefen A. Computer modeling studies to assess whether a prophylactic dressing reduces the risk for deep tissue injury in the heels of supine patients with diabetes. *Ostomy Wound Manag* 2016;62(4):42–52.
24. Burton JN, Fredrickson AG, Capunay C, Tanner L, Oberg C, Santamaria N, Gefen A, Call E. Measuring tensile strength to better establish protective capacity of sacral prophylactic dressings over 7 days of laboratory aging. *Adv Skin Wound Care* 2019 Jul;32(7S Suppl 1):S21–S27.
25. Burton JN, Fredrickson AG, Capunay C, Tanner L, Oberg C, Santamaria N, Gefen A, Call E. New clinically relevant method to evaluate the life span of prophylactic sacral dressings. *Adv Skin Wound Care* 2019 Jul;32(7S Suppl 1):S14–S20.
26. Gefen A, Alves P, Creehan S, Call E, Santamaria N. Computer Modeling of prophylactic dressings: an indispensable guide for healthcare professionals. *Adv Skin Wound Care* 2019 Jul;32(7S Suppl 1):S4–S13.
27. Santamaria N, Gerdtz M, Sage S, McCann J, Freeman A, Vassilou T, DeVincentis S, Wei A, Manias E, Liu W, Knott J. A randomized controlled trial of the effectiveness of soft silicone foam multi-layer dressings in the prevention of sacral and heel pressure ulcers in trauma and critically ill patients: the border trial. *Int Wound J* 2015;12(3):302–308.
28. Kalowes P, Messina V, Li M. Five-layered soft silicone foam dressing to prevent pressure ulcers in the intensive care unit. *Am J Crit Care* 2016;25(6):e108–e119.
29. Santamaria N, Gerdtz M, Liu W, Rakis S, Sage S, Ng AW, Tudor H, McCann J, Vassiliou T, Morrow F, Smith K, Knott J, Liew D. Clinical effectiveness of a silicone foam dressing for the prevention of heel pressure ulcers in critically ill patients: border II trial. *J Wound Care* 2015;24(8):340–345.
30. Call E, Pedersen J, Bill B, Oberg C, Ferguson-Pell M. Microclimate impact of prophylactic dressings using in vitro body analog method. *Wounds* 2013;25(4):94–103.
31. Hayden JK, Cole JB. The effectiveness of a pain wrap compared to a standard dressing on the reduction of post-operative morbidity following routine knee arthroscopy: a prospective randomized single-blind study. *Orthopedics* 2003;26(1):59–63.
32. McGuinness W, Vella E, Harrison D. Influence of dressing changes on wound temperature. *J Wound Care* 2004;13(9):383–385.
33. Zeevi T, Levy A, Brauner N, Gefen A. Effects of ambient conditions on the risk of pressure injuries in bedridden patients—multi-physics modelling of microclimate. *Int Wound J* 2017;15(3):402–416.
34. Gefen A. Managing inflammation by means of polymeric membrane dressings in pressure ulcer prevention. *Wounds Int* 2018;9:22–28.
35. Labview ver. 7.2, 2005. <http://www.ni.com/en-il.html>
36. Simpleware® Ltd. ScanIP, +FE, +NURBS and +CAD Reference Guide ver. 5.1, 2012. <http://www.simpleware.com/software/>
37. ABAQUS 2017® Ltd. 2017. <http://www.3ds.com/products-services/simulia/products/abaqus/>
38. Linder-Ganz E, Shabshin N, Itzhak Y, Gefen A. Assessment of mechanical conditions in sub-dermal tissues during sitting: a combined experimental-MRI and finite element approach. *J Biomech* 2007;40(7):1443–1454.
39. Palevski A, Glaich I, Portnoy S, Linder-Ganz E, Gefen A. Stress relaxation of porcine gluteus muscle subjected to sudden transverse deformation as related to pressure sore modeling. *J Biomech Eng* 2006;128(5):782–787.
40. Gefen A, Haberman E. Viscoelastic properties of ovine adipose tissue covering the gluteus muscles. *J Biomech Eng* 2007;129(6):924–930.
41. Peko Cohen L, Levy A, Shabshin N, Neeman Z, Gefen A. Sacral soft tissue deformations when using a prophylactic multilayer dressing and positioning system. *Journal of wound, ostomy and continence. Nursing* 2018;45(5):432–437.
42. Fiala D, Lomas KJ, Stohrer M. A computer model of human thermoregulation for a wide range of environmental conditions: the passive system. *J Appl Physiol* 1999;87(5):1957–1972.
43. Fiala D, Lomas KJ, Stohrer M. Computer prediction of human thermoregulatory and temperature responses to a wide range of environmental conditions. *Int J Biometeorol* 2001;45(3):143–159.
44. Pennes HH. Analysis of tissue and arterial blood temperatures in the resting human forearm. *J Appl Physiol* 1948;1:93–122.
45. Fiala D, Havenith G, Bröde P, Kampmann B, Jendritzky G. UTCI-Fiala multi-node model of human heat transfer and temperature regulation. *Int J Biometeorol* 2011;56(3):429–441.
46. Prasad K, Kramer R, Marsh N, Nyden M, Ohlemiller T, Zammarano M. Numerical simulation of fire spread on polyurethane foam slabs. In Fire Research Division, BFRL, NIST Annual Fire Conference, 2009
47. Jarfelt U, Olle R. Thermal conductivity of polyurethane foam—best performance. 10th International Symposium on district heating and cooling. Chalmers University of Technology Goteborg, Sweden, 2006.
48. Call E, Pedersen J, Bill B, Black J, Alves P, Brindle CT. Enhancing pressure ulcer prevention using wound dressings: what are the modes of action? *Int Wound J* 2015;12(4):408–413.
49. Patel S, Knapp CF, Donofrio JC, Salcido R. Temperature effects on surface pressure-induced changes in rat skin perfusion: implications in pressure ulcer development. *J Rehabil Res Dev* 1999;36(3):189–201.
50. Thirumal M, Khastgir D, Singha N, Manjunath B, Naik Y. Effect of foam density on the properties of water blown rigid polyurethane foam. *J Appl Polym Sci* 2008;108(3):1810–1817.
51. Bhargava A, Chanmugam A, Herman C. Heat transfer model for deep tissue injury: a step towards an early thermographic diagnostic capability. *Diagn Pathol* 2014;9:36.
52. Jan Y, Lee B, Liao F, Foreman R. Local cooling reduces skin ischemia under surface pressure in rats: an assessment by wavelet analysis of laser Doppler blood flow oscillations. *Physiol Meas* 2012;33(10):1733–1745.
53. Lachenbruch C. Skin cooling surfaces: estimating the importance of limiting skin temperature. *Ostomy Wound Manage* 2005;51(2):70–79.

54. Kokate JY, Leland KJ, Held AM, et al. Temperature-modulated pressure ulcers: a porcine model. *Arch Phys Med Rehabil* 1995; 76(7):666–673.
55. Fluhr JW, Darlenski R, Surber C. Glycerol and the skin: holistic approach to its origin and functions. *Br J Dermatol* 2008;159:23–34.
56. Saegeman VS, Ectors NL, Lismont D, Verduyck B, Verhaegen J. Short- and long-term bacterial inhibiting effect of high concentrations of glycerol used in the preservation of skin allografts. *Burns* 2008 Mar;34(2):205–211.

**How to cite this article:** Schwartz D, Gefen A. An integrated experimental-computational study of the microclimate under dressings applied to intact weight-bearing skin. *Int Wound J*. 2020;17:562–577. <https://doi.org/10.1111/iwj.13309>